LCLS-TN-99-6
SLAC-PUB-8053
February 1999

The LCLS X-ray FEL at SLAC

M. Cornacchia

Invited talk presented at SPIE Photonic West 99; Free-Electron Laser Challenges, 1/23/99ã1/29/99, San Jose, CA, USA

Stanford Linear Accelerator Center, Stanford University, Stanford, CA 94309

Work supported by Department of Energy contract DE AC03 76SF00515.

SLAC-PUB-8053
February 1999

The LCLS X-RAY FEL at SLAC

M. Cornacchia*, Stanford Linear Accelerator Center, MS16, Stanford, CA 94309

ABSTRACT

The design status and R&D plan of a 1.5 Å SASE-FEL at SLAC, called the Linac Coherent Light Source (LCLS), are described. The LCLS utilizes one third of the SLAC linac for the acceleration of electrons to about 15 GeV. The FEL radiation is produced in a long undulator and is directed to an experimental area for its utilization. The LCLS is designed to produce 300 fsec long radiation pulses at the wavelength of 1.5 Å with 9 GW peak power. This radiation has much higher brightness and coherence, as well as shorter pulses, than present 3rd generation sources. It is shown that such leap in performance is now within reach, and is made possible by the advances in the physics and technology of photo-injectors, linear accelerators, insertion devices and free-electron lasers.

Keywords: Free-Electron Laser, Particle Accelerator, Light Source, Synchrotron Radiation.

1. INTRODUCTION

At the Photonic West `97 Conference a report was given[1] on the proposal to build a Free-Electron Laser at the Stanford Linear Accelerator Center (SLAC). This paper is a report on the progress of the project since then. Several successful milestones have marked two years of work.

A multi-laboratory collaboration was formed with the scope to build the LCLS using the last 1/3 of the SLAC linac, starting in the year 2002[2]. The collaboration includes that Stanford Synchrotron Radiation Laboratory, a division of the Stanford Linear Accelerator Center (SLAC), other divisions of SLAC, Argonne National Laboratory, Lawrence Livermore National Laboratory, Los Alamos National Laboratory and the University of California at Los Angeles.

The LCLS collaboration produced a Design Study[3] that was validated by an internationally-constituted Director's Review at SLAC in November, 1997 and that proved the feasibility of the concept. It moreover confirmed the extraordinary projected performance of the LCLS, which represents an increase of approximately ten orders of magnitude in peak brightness, and three orders of magnitude in average brightness, over 3rd generation sources like the APS and ESRF. Even without the FEL amplification this linac-based radiation source would produce spontaneous undulator radiation at 1.5 Å with subpicosecond pulse duration, whose peak brightness would be four orders of magnitude larger than the best undulator at APS and ESRF.

This paper is organized as follows. Section 2 briefly recalls the mechanism of the Self-Amplified-Spontaneous-Emission (SASE). Section 3 gives an overview of the LCLS layout. Section 4 discusses the performance characteristics. In Section 5 we describe the various components of the LCLS and the electron and photon beam characteristics and requirements in the various stages of electron bunch formation and acceleration, FEL radiation generation and x-ray optics. In Section 6 we report on the status of the experimental studies on SASE. Section 7 contains a summary and plan for the construction of the facility.

The scientific applications of the LCLS are not covered in this report.

2. PRINCIPLE OF OPERATION

In present Free-Electron Lasers the light from many passes of the electron beam is stored in an optical cavity formed by mirrors. Mirrors, however, becomes less and less efficient at shorter wavelengths, less than ~2000 Å.

The LCLS is based on the Self-Amplified-Spontaneous-Emission (SASE) principle, proposed[4,5] and analyzed for short wavelengths FELs[6]. In the SASE mode of operation, high power transversely coherent, electromagnetic radiation is produced from a single pass of a high peak current electron beam through a long undulator, and no mirrors are needed as in optical cavities. The electron beam, describing an oscillatory trajectory in the undulator, interacts with the transverse electric field of the radiation; the interaction produces an energy modulation at the wavelength $\lambda = \lambda_u \left(1 + k^2\right) / 2 \Big/ 2\gamma^2$ where λ_u is the

* Correspondence: Email: cornacchia@ssrl.slac.stanford.edu; Telephone: 650 926 3906; Fax: 650 926 4100

undulator period and K the undulator parameter[7]. The electron energy modulation modifies the electron trajectory in the undulator in such a way as to produce bunching at the scale λ. The electrons bunched within a optical wavelength all emit radiation that is in phase, ie the intensity of the radiation is proportional to the square of the number of electrons cooperating, rather than increasing only linearly with the number of electrons, as is the case with normal synchrotron radiation. The electromagnetic field creates more energy modulation and bunching, leading to exponential growth of the radiation. Due to non-linear effects, the radiation growth saturates after a certain length along the undulator, corresponding to about 10 field gain lengths.

The LCLS proposes to achieve the Angstrom range with an electron beam energy of 14.3 GeV, a peak current of 3.4 kA, low emittance (1.5 π mm-mrad), small energy spread (0.02%) and a long undulator (100 m). These rather strict conditions on the beam quality are imposed by the following conditions[8]:

- For the beam transverse emittances, $\varepsilon \approx \lambda / 4\pi$.
- For the energy spread in a cooperation length (l_c), $\sigma_E / E < \rho$, where ρ is the FEL parameter = $\left[K\Omega_p f_b / (4\gamma\omega_u) \right]^{2/3}$, $\omega_u = 2\pi c / \lambda_u$ is the frequency associated to the undulator periodicity and $K = eB_u\lambda_u / (2\pi mc^2)$ (cgs units). $\Omega_p = \left(4\pi r_e c^2 n_e / \gamma \right)^{1/2}$ is the beam plasma frequency, n_e is the electron density, r_e is the classical electron radius and f_B is the Bessel function factor. B_u is the undulator peak magnetic field, mc^2 the electron's rest energy. The cooperation length is $l_c = \lambda / (4\pi\rho)$.
- For the undulator length, $N_u\lambda_u \approx 10L_g$, where L_g is the field gain length, $L_g \approx \lambda_u / (2\pi\sqrt{3}\rho)$.
- The radiation gain length must be shorter than the radiation Raleigh range, $L_g < L_R$, where $L_R = \pi w_0^2 / \lambda$ and w_0 is the radiation beam radius.

3. OVERALL LAYOUT

Fig. 1 shows the layout of the proposed facility. The hexagonal shape at the end of the linac is the PEP-II *B* Factory electron-positron collider that uses the first 2 km of the Linear Accelerator as the injector. The last 1 km of the linac will be used by the LCLS.

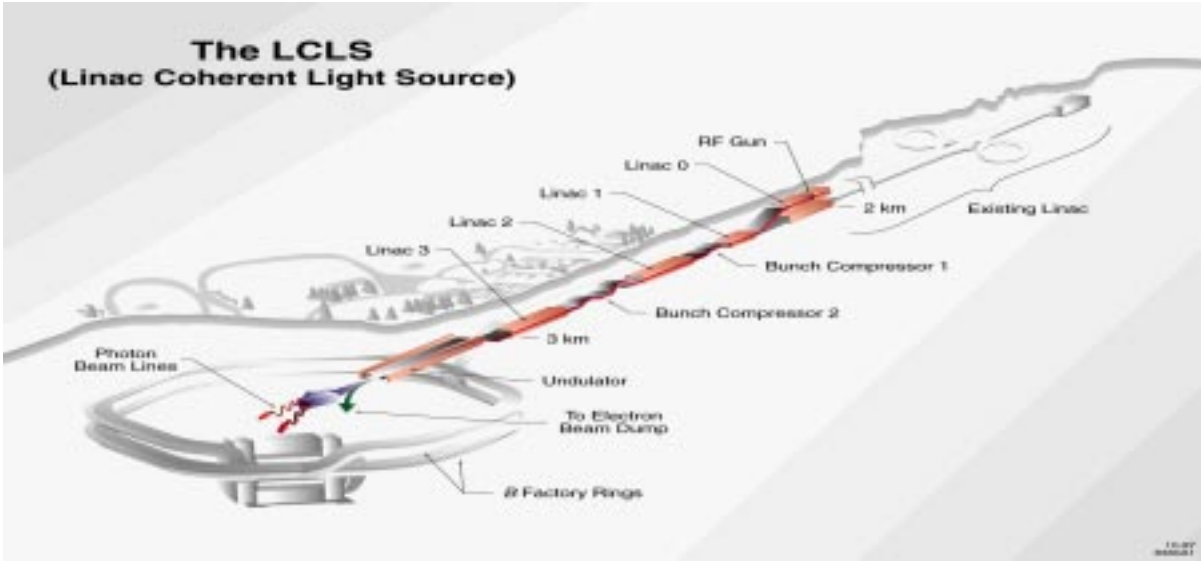

Fig. 1. Layout of the Linac Coherent Light Source.

A new injector consisting of a gun and a short linac is used to inject an electron beam into the last kilometer of the SLAC linac. With the addition of two stages of magnetic bunch compressor, the electron beam exits the linac with an energy of 14.3 GeV, a peak current of 3,400 A, and a normalized emittance of 1.5π mm-mrad. A transfer line takes the beam and matches it to the entrance of the undulator. The 100 m long undulator will be installed in the tunnel that presently houses the Final Focus Test Beam (FFTB). After exiting the undulator, the electron beam is deflected onto a beam dump, while the photon beam enters the experimental areas.

4. PERFORMANCE CHARACTERISTICS

The main parameters are shown in Table 1.

Table 1. Main LCLS parameters

Parameters	**Value**	**Units**
Electron Beam Energy	14.35	GeV
Emittance	1.5	π mm-mrad
Peak current	3,400	A
Energy spread (uncorrelated)	0.006	%, rms
Energy spread (correlated)	0.10	%, rms
Bunch length	67	fsec, rms
Undulator period	3	cm
Number of undulator periods	3,328	
Undulator magnetic length	99.8	m
Undulator field	1.32	Tesla
Undulator gap	6	mm
Undulator parameter, K	3.7	
FEL parameter, ρ	4.7×10^{-4}	
Field gain length	11.7	m
Repetition rate	120	Hz
Saturation peak power	9	GW
Peak brightness	$1.2 \times 10^{32} - 1.2 \times 10^{33}$	Photons/(s mm^2 mrad^2 0.1% bandwidth)
Average brightness	$4.2 \times 10^{21} - 4.2 \times 10^{22}$	Photons/(s mm^2 mrad^2 0.1% bandwidth)

Fig. 2 shows the average and peak brightness as a function of the photon energy for the LCLS and other operating facilities. It indicates that the peak brightness of the LCLS would be about ten orders of magnitude greater than currently achieved in 3rd generation sources. The peak spontaneous emission alone (independent of the laser action) if four orders of magnitude greater than in present sources. Even the average brighness, though limited by the low repetition rate of the linac, is still orders of magnitude higher than the brightest synchrotron radiation sources. The sub-picosecond pulse length is two orders of magnitude shorter than can be achieved in a synchrotron. The FEL radiation has full transverse coherence. Longitudinally, the radiation is delivered in wave-trains[9]. The wave-trains are uncorrelated, in phase and amplitude, from each other. The longitudinal coherence is therefore defined by the relative bandwidth of the wave-train, which, at saturation, is approximately[8] $1/N_u \sim \rho = 4.7 \times 10^{-4}$.

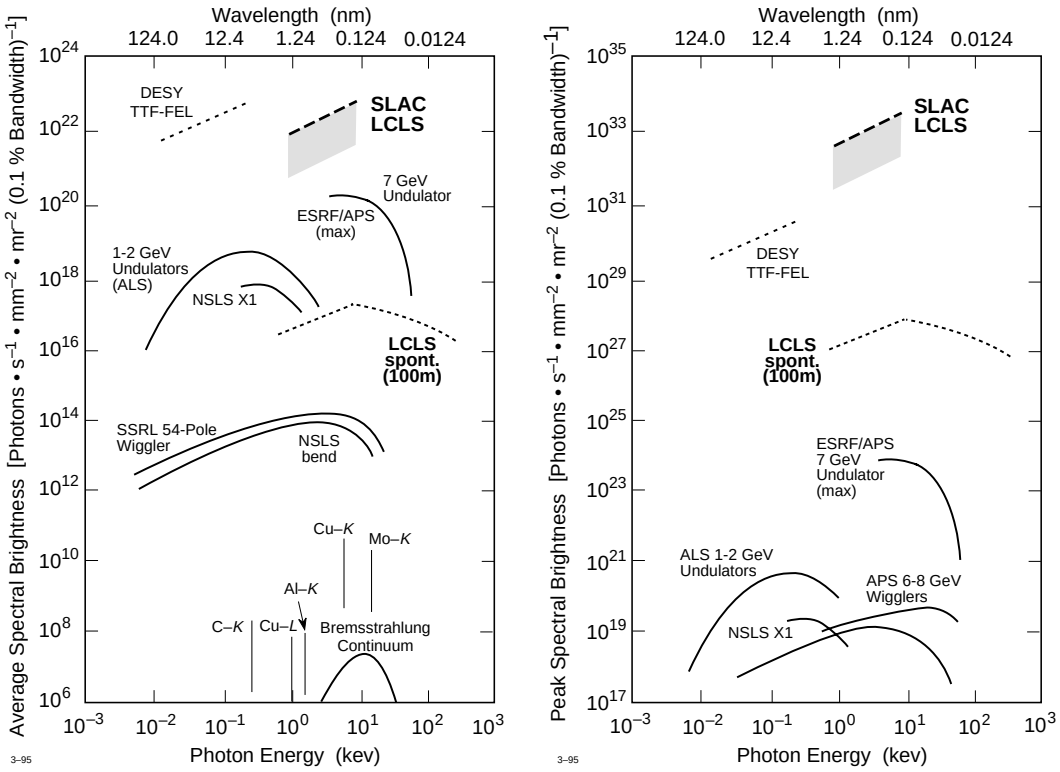

Fig. 2. Average and peak brightness calculated for the LCLS and for other facilities operating or under construction.

The output of the radiation is shown Fig. 3, which is the result of simulation with the code GINGER[10]. The radiation builds up exponentially along the undulator, reaching saturation at about 90 m. The zoom on the microstructure shows the spiky nature of the radiation and the "clean-up" of the spectrum as saturation is approached. The radiation is emitted as a temporal sequence of regions where it peaks. The length of each region is of the scale of $2\pi L_c$[11] , where L_c is the coherence length, defined as the slippage between the electron beam and the radiation in a gain length ($L_g\lambda_r/\lambda_u$).

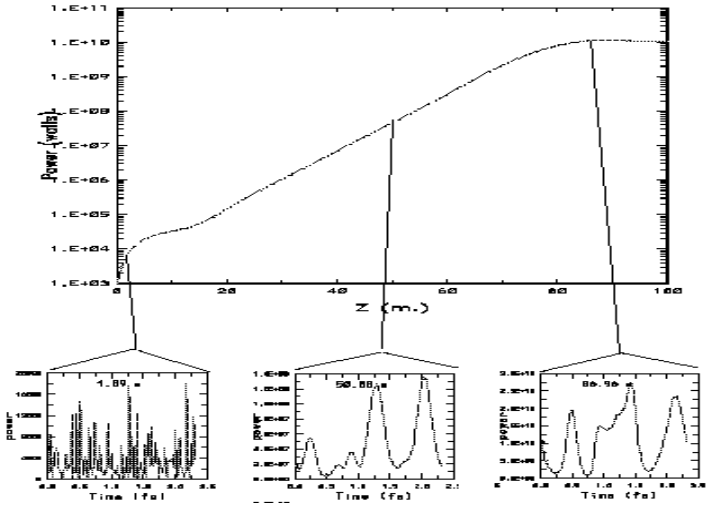

Fig. 3. Build-up of the radiation along the undulator length. The zoom on the microstructure shows the details of the radiation spikes.

The spectrum of the radiation consists of sharp peaks centered around the 1st and 3rd FEL harmonics and of the spontaneous radiation. The latter extends to several hundred keV, as shown in Fig. 4.

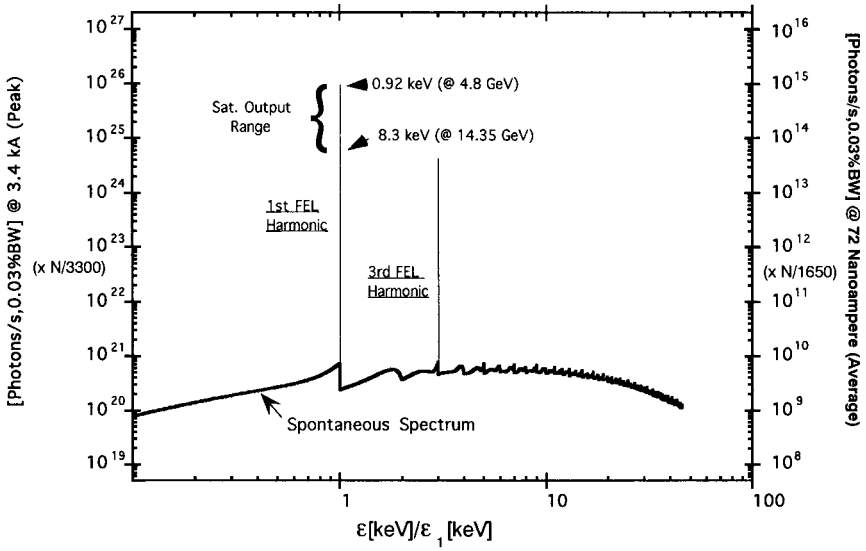

Fig. 4. Average and peak coherent and spontaneous spectral fluxes. N is the number of periods, ε_1 is the fundamental FEL harmonic (0.92 keV at 4.8 GeV and 8.3 keV at 14.35 GeV).

5. DESCRIPTION OF THE COMPONENTS OF THE LCLS

It should be apparent, from the description given so far and the parameters of Table 1, that in order to achieve lasing at the shortest wavelength, 1.5 Å, the brightness of the electron source must be high. The electron beam emittance is small, 1.5π mm-mrad (rms and normalized), the electron bunch is compressed to an rms length of 67 fsec before entering the undulator, and the peak current is high, 3,400 A. These specifications would have been beyond reach 10 or 15 years ago. It is a fortunate development for x-ray FELs that several advances took place over the last decade in the technology of high-brightness electron beams. These are the research and development effort on linear colliders, the commissioning, operation and experimental studies of the SLAC Linear Collider (SLC) and FFTB, and the parallel effort on the development of radio-frequency photo-injectors. The remarkable progress in these fields, together with the advances in the technology of insertion devices, make it now possible to design and construct an x-ray free-electron laser.
In this section we discuss some of the characteristics of the LCLS components and a choice of parameters that meet the FEL requirements.

5.1 The Photo-injector

The injector is required to produce a single 150 MeV bunch of ~ 1 nC charge and ~ 100 A peak current at a repetition rate of 120 Hz with a normalized rms transverse emittance (horizontal and vertical) of ~ 1 π mm-mrad. This is the emittance defined along a small "slice" of the electron bunch. The adjective "small" applies to a fraction of the bunch length of the order of the correlation length (0.3 μ at 1.5 Å). A slice emittance of 1.4 π mm-mrad at 1 nC has already been obtained[12]. The design employs a solenoidal field near the cathode of the rf gun. The initial projected emittance growth due to space charge is almost completely compensated[13] at the end of the booster linac (Linac 0 in Figs. 1 and 6). This is shown in Fig. 5, that depicts the simulation of the evolution of the normalized emittance[14] from the gun cathode to 150 MeV. These simulations show that this design will produce the desired emittance. Spacial and temporal shaping of the laser pulse will further reduce the compensated emittance.

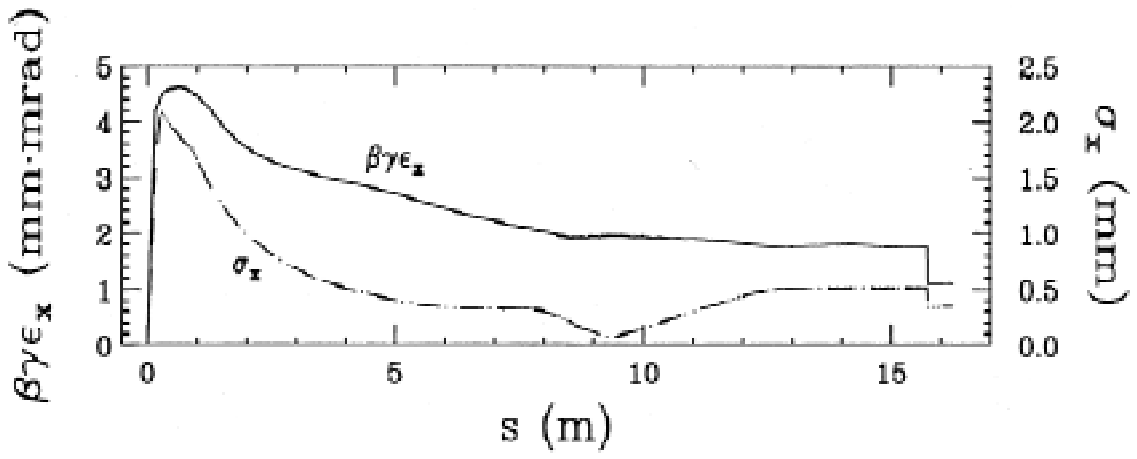

Fig. 5. Normalized emittance (solid line) and rms beam size (dashed line) along the beamline from the cathode (s=0) to 150 MeV at the end of the linac. The step at ~16 m is a 7.7% halo cut.

In addition to the low emittance, there are two additional electron beam requirements that pose a challenge: the timing and intensity stabilities should have an rms value of < = 0.5 ps and < = 1% respectively. These tolerances are needed to insure optimum compression condition and are determined essentially by the laser system. Commercial laser oscillators are available with a timing stability of 0.5 ps and this stability is already routine in the SLC. The laser will have a Nd:YLF or YAG-pumped Ti-Sapphire amplifier operating at 750 nm that will be frequency tripled.

5.2 Compression and Acceleration

For operation at 1.5 Å an electron peak current of 3,400 A with a transverse emittance of 1.5 π at 14.3 GeV is required. With these parameters the length of the undulator that will give lasing with a comfortable margin for field errors and misalignments is ~ 112 m, which is also the maximum length that can be fitted in the FFTB tunnel[15]. Since the photo-injector can produce 1 nC in 3 a ps long bunch, corresponding to a peak current of 100 A, the bunch has to be compressed 30 times to reach the peak current of 3,400 A required for lasing. The layout of the compression and acceleration is shown in Fig. 6.

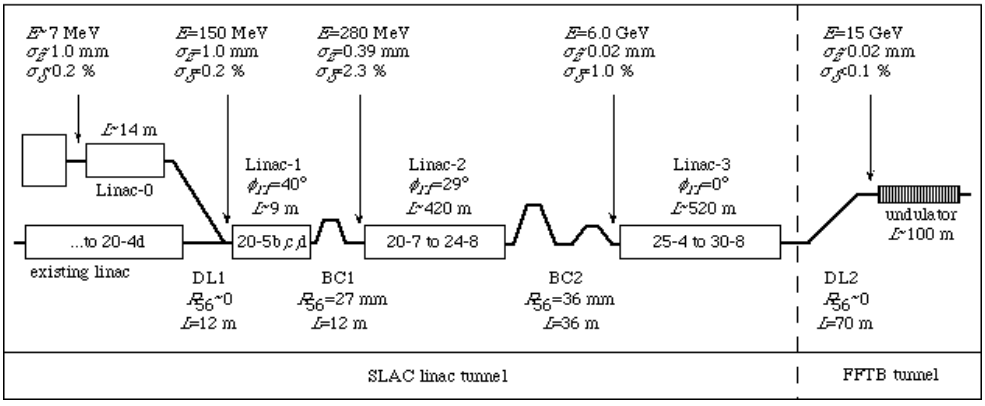

Fig. 6. LCLS bunch compression and acceleration schematic.

The dog legs (DL1 and DL2) are simple transport lines and have no effect on the bunch length. BC1 is the first compressor chicane. BC2 is the second compressor and consists of a double chicane. The chicanes are arranged such that the non-linearities in the compression and acceleration process (longitudinal wake-fields, rf curvature and second order momentum

compaction) are partially cancelled. The choice of parameters compensates the correlated energy spread after the final compression and desensitizes the system to phase and charge variations. The energy of the first compressor is 280 MeV, set by the need to minimize space charge effects at low energy, while the upper limit is set by the desire to compress the bunch early in the linac to ease transverse wake-fields. In the first compressor the bunch shrinks from 1 mm to 390 μm rms. After the second compressor the bunch length is only 20 μm. The energy of the second compressor, 6 GeV, is set by the conflicting requirements of longitudinal emittance dilution due to synchrotron radiation effects and longitudinal wake-fields. The second compressor (BC2) is asymmetric, with the last two dipoles having a weaker field to avoid the emittance blow up induced by the coherent synchrotron radiation emitted in the bends where the bunch is shortest[16]. Since the energy spread introduced by the coherent synchrotron radiation is correlated along the bunch, its effect on the transverse emittance is minimized by introducing a double chicane and optical symmetry to cancel the longitudinal-to-transverse coupling. With this scheme the simulations indicate that the emittance blow up due to coherent synchrotron radiation is of the order of 3-5 %.

The effect of emittance blow up on the FEL performance depends on whether the blow up is over a small (~0.3 μm, ie of the order of the correlation length) slice of the 20 μm bunch or whether it is correlated along the length of the bunch (projected emittance). The former affects the lasing action and the saturation length, whereas the latter only leads to a reduction of brightness. With all the dynamics effects included, the simulations performed with the code LIAR[17] indicate that the projected emittance blow up at the entrance of the undulator is in the range 20-50 %, depending on how the various dilutions add. The design assumes a slice emittance blow up of 50%, ie a slice emittance of 1.5 π mm-mrad in determining the length of the undulator. This is a conservative estimate since, as we have shown, most dilution mechanisms affect the projected rather than the slice emittance.

Various factors contribute to a blow up of the longitudinal energy spread. These can be incoherent (intrinsic spread and the effect of incoherent synchrotron radiation) or correlated along the bunch (geometric wake, coherent synchrotron radiation, resistive wall, wakes driven by surface roughness). The simulations[18] indicate that the former is about 0.02%, while the correlated energy spread is smaller than 0.1%. The theory and simulation of the FEL lasing dynamics indicate that these number are quite acceptable. The incoherent (slice) spread is smaller than the FEL parameter ρ (4.7×10^{-4}), thus verifying one of the conditions of Section 2. The energy spread correlated along the bunch does not affect the FEL action, and leads to a brightness dilution that was included in the calculations.

5.3 The undulator

The SASE-FEL theory developed over the last fifteen years[19] provides the understanding of the process and of the interplay amongst the various FEL parameters. For a more precise determination of the requirements and performance, three dimensional studies have been carried out with computer codes[20] and a parametric formula[21]. Details of this study can be found in Chapter 5 of the LCLS Design Report[3]. The undulator parameters are given in Table 1. After reviewing several possible magnet designs, a planar Halbach hybrid type was adopted, with a period of 30 cm and a fixed 6 mm magnetic gap. The poles are made of vanadium permendur, and the magnets that drive them will be made of NdFeB.

The undulator was optimized in terms of its focusing lattice and strength. The eletron optics consists of FODO cells, with a cell length of 4.32 m. Focusing is obtained by placing permanent magnet quadrupoles in the interruptions of the undulator sections. Each interruption is 23.5 cm long, and also includes beam position monitors and vacuum ports. It was found, theoretically[22] and through computer studies, that such interruptions are harmless to the FEL process. Fig. 7 shows a schematic side view of the undulator structure, showing the FODO lattice with the 1.92 m separations for diagnostics, focusing correctors and vacuum ports. The undulator magnets are mounted on aluminum girders whose temperature is stabilized.

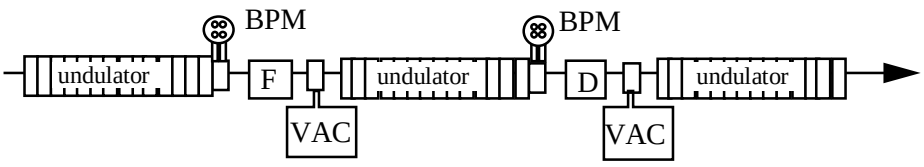

Fig. 7 . Schematic view of undulator structure.

The corrections to the electron orbit are obtained by a small lateral displacement of the quadrupoles; the total movement is 0.5 mm with a resolution of 1 μm. The electron beam trajectory is required to be straight to within 5 μm over a field gain length (11.7 m) to achieve adequate overlap between the electron and photon beams. The excellent resolution of monitors of choice (microwave type detectors), better than 1 μm, is not sufficient to satisfy the requirements for absolute orbit correction, since this requires the knowledge of the absolute position of the monitors with the same order of accuracy as the electron beam straightness. This absolute accuracy is not achievable with present mechanical alignment techniques. Fortunately, a beam based alignment method, already in use at the SLC and FFTB, offers a solution to this problem. Without putting very tight tolerances on absolute physical BPM alignment, the technique provides information about BPM position and gain errors that can be used to correct the readings so that the electron beam trajectory deviation from a straight line can be measured down to a few microns. The technique uses BPM readings as a function of large, deliberate variations in the electron energy. The measured are analyzed and then converted to (a) quadrupole magnet transverse position corrections, (b) BPM offset corrections and (3) adjustments of the incoming beam position and angle at the undulator entrance. The alignment procedure is repeated 2-3 times in succession for the initial machine start up, and then reapplied only once per few weeks as necessary. Once the absolute position of the BPMs has been determined, a simple steering technique will be used for daily trajectory control, and a fast feedback system will keep the trajectory stable in a time scale of seconds. A detailed description of the method can be found in the LCLS Design Report[23]. The simulations that have been performed to verify the method include all conceivable errors of the BPMs and quadrupoles, and show that the absolute position of the trajectory can be made to be straight to within 5 μm with only two iterations.

Because of the high peak electron current and the small radius (2.5 mm) of the undulator pipe, wake-field effects have to be considered. The resistive wall effects can be made small by plating the stainless steel chamber with copper. Roughness of the beam pipe surface may cause a momentum spread increase[24] that reduces the FEL performance if it is greater than about 100 nm. With some R&D effort, this smoothness is achievable. Fig. 8 shows the effect of the resistive wall and roughness induced wake-fields on the momentum deviation along the bunch length at the end of the undulator. Since the energy deviation increases linearly along the undulator, it interferes with the longitudinal dynamics of the FEL process. The simulations indicate that the maximum energy deviation should be kept below 0.1% in order not to reduce the FEL performance in terms of saturation length and brightness. In Fig. 8, the charge distribution along the bunch, f(z), is derived from tracking the bunch in the linear accelerator and, as can be seen, is clearly non-gaussian. Just 55% of the electrons are altered in energy by less than ± 0.1%.

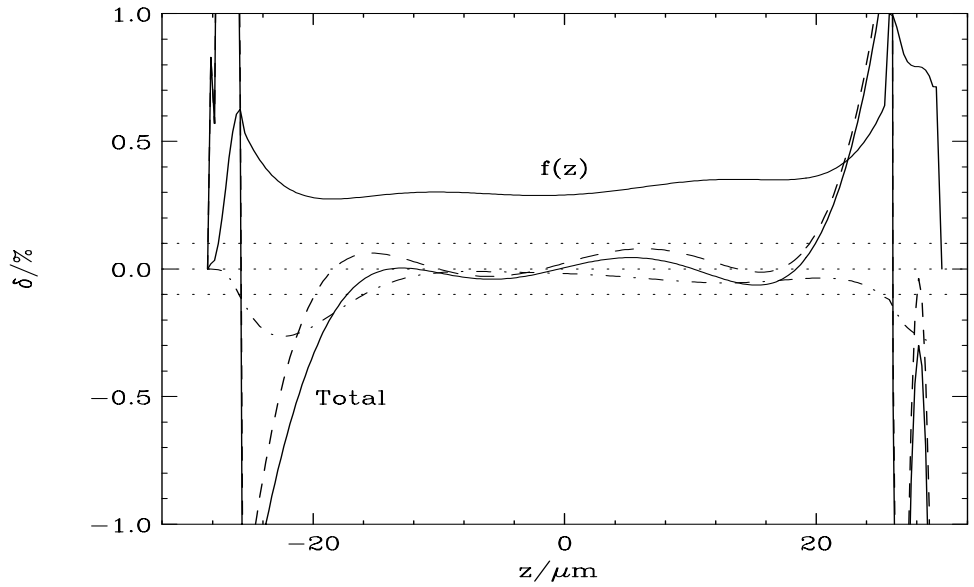

Fig. 8. Roughness (dash), resistive wall (dotdash) and total (solid) wake-field generated within the 112-meter undulator for the distribution f(z). A copper surface and a roughness of 100 nm is assumed. The bunch head is at the left.

5.4 The Output Radiation and the Undulator-to-Experimental Area Transport

The coherent output of the LCLS features peak output powers in the 10 GW range, average powers of the order of 1 W, spectral bandwidth of the order of 0.1%, full transverse coherence and pulse lengths of approximately 300 fs. The total peak power of the spontaneous radiation is 80 GW, thus largely exceeding the power of the coherent FEL output. The peak on-axis power density of the spontaneous radiation is 10^{13} W/cm^2 (at 1.5 Å), approximately one hundred times smaller than that of the coherent line, which, due to its full transverse coherence can, in principle, be focused to an approximate limit of 10^{25} W/cm$^{2.}$. In the initial operation it is expected that the high peak power and power density will inhibit the utilization of the full FEL flux with conventional focusing and transport optics. On the other hand, there will be a unique opportunity to study the effect of high peak power density on materials and optical elements, thereby opening the path to the full exploitation of the radiation in the LCLS and other future facilities.

After the beam has exited the undulator, an absorption cell intercepts the radiation; its purpose is to attenuate the power to levels manageable with conventional optics and to provide a continuous transition to power densities at which meaningful research on the interaction of LCLS-type pulses with matter can proceed. The coherent FEL radiation will be separated from the spontaneous radiation by the absorption cell, by spectral and angular filters made of mirrors or crystals, and by horizontally/vertically tunable x-ray slits. The bremsstrahlung radiation, a concern for both personnel safety and experimental noise, will be absorbed by a mirror or crystal, while the thermal neutrons created by this interaction will be stopped by a lead/polyethylene shield wall. The absorption cell is used to vary the output power of the radiation. Alternatively, a long beam line (780 m) could be built to reduce the beam's power density without diluting its brightness. The Experimental Hall will consist, initially, of one crystal and one mirror beamline.

6. EXPERIMENTAL STUDIES OF SASE-FELs

Several experiments in recent years are providing confidence that the theory and the computations used to design the LCLS are reliable. The first experimental results on SASE were obtained in the microwave region[25], with gains of the order of 10^6-10^7. Over the last couple of years, experiments in the infrared and visible region obtained gains of one to two orders of magnitude[26] and, more recently, a gain of 3×10^5 was obtained at 12 μm[27]. In this experiment the gain length and output power fluctuations were measured, giving results in very good agreement with theory and simulations. Although these results are encouraging and are providing, together with the theory and the simulations, already a solid basis for the LCLS design, they have not yet reached the saturation regime, where the LCLS and other future facilities will operate. For this reason, more experiments are being planned to further study the SASE-FEL physics at saturation and shorted wavelengths. A BNL-LANL-LLNL-SLAC-UCLA group is working on a 0.6-0.8 μm experiment to be carried out at the Accelerator Test Facility at NSLS/BNL in 1999. The experiment will use a 4 m long undulator with distributed strong focusing. It will reach saturation and will study the radiation time structure and angular distribution. Other experiments are planned at NSLS/BNL (harmonic generation in the infrared to visible and SASE in the region 1-0.2 μm) and at APS/ANL (0.5-0.1 μm). At DESY, construction is underway for a 420 Å SASE-FEL that will use the TESLA Test Facility superconducting linac, with the first operation expected in 1999. In phase 2, scheduled around 2003, the wavelength will go down to 60 Å[28].

7. SUMMARY

The LCLS would create a photon beam of unprecedented brightness, coherence, beam power and short pulses, far surpassing anything available in 3rd generation sources. It will use, for the most part, existing components, techniques and facilities available at SLAC. The plan envisages 2 years of research and development (2000-2001), after which construction could start in FY2002.

ACKNOWLEDGMENTS

The author wishes to thank all the colleagues with have contributed to the LCLS Design Study,[29] and on whose work this paper is based.

This report was prepared for the Department of Energy under contract number DE-AC03-76SF00515 by Stanford Linear Accelerator Center, Stanford University, Stanford, California.

[1] M. Cornacchia et al. , "Performance and Design Concepts of a Free Electron Laser Operating in the X-ray Region", Proceedings of Photonic West `97 Conference, 8-14 February, 1997, San Jose`, CA, publication No. 2988-01.
[2] The first 2/3 of the SLAC linac is used for injection into the PEP-II B-Factory. This leaves the last 1/3 free for acceleration to 15 GeV.
[3] LCLS Design Study Report, SLAC Publication R-521 and UC-414.
[4] R. Bonifacio, C. Pellegrini, L.M. Narducci, *Opt. Commun.* "Collective instabilities and high gain regime in a free-electron laser", Vol. 50, No. 6 (1985); J.B. Murphy, C. Pellegrini, "Generation of high intensity coherent radiation in the soft x-ray and VUV regions", *Jour. Opt. Soc. Of Ameri., B2, 259 (1985).*
[5] Y. S. Derbenev, A.M. Kondradenko and E.L. Saldin, *Nul.r Instr. and Meth*, A193, 415 (1982).
[6] K.-J. Kim *et al.*, "Issues in storage ring design for operation of high gain FELs", *Nucl. Inst. and Meth. In Phys. Res. A239*, 54 (1985); K.-J. Kim, "Three-dimensional analysis of coherent amplification and self-amplified spontaneous emission in free-electron lasers", *Phys. Rev. Letters*, Vol. 57, 1871 (1986); c. Pellegrini, "Progress towards a soft x-ray FEL", *Nucl. Inst. And Meth. In Phys. Res.* A272, 364 (1988).
[7] See, for instance, P. Elleaume, "Free electron laser undulators, electron trajectories and spontaneous emission" in *Laser Handbook*, Vol. 6, pp. 91-114, W.B. Colson, C Pellegrini and A. Renieri editors, North-Holland, 1990.
[8] J.B. Murphy and C. Pellegrini, "Introduction to the Physics of the Free-Electron Laser", in *Laser Handbook*, Vol. 6, pp.9-70, W.B. Colson, C. Pellegrini and R. Renieri eds., North-Holland, 1990.
[9] R. Bonifacio et al.,"Spectrum temporal structure and fluctuations ina high gain free electron laser starting from noise", *Phys. Rev. Lett. 73*, p. 70 (1994).
[10] R.A. Jong, W.M. Fawley and E.T. Scharlemann,"Modelling of Induction-Linac Based Free-Electron Laser Amplifiers", in *Modelling and Simulations of Laser Systems, Proc. SPIE* **1045**, pp.18-27, 1989.
[11] R. Bonifacio *et al.*, "Spectrum, Temporal Structure and Fluctuations in a High-Gain Free-Electron Laser Starting from Noise", *Phys. Rev. Let.*, **73**(1), p. 70, 1994.
[12] M. Babzien et al."Observation of Self-Amplified Spontaneous Emission in the Near-Infrared and Visible Wavelength", *Phys. Rev.* **E 57** (6093), 1998.
[13] B.E. Carlsten, *Nucl. Instrum. and Meth. A 285* (1989) 313.
[14] The simulations were performed with the computer code PARMELA.
[15] The magnetic length of the undulator is 99.8 m. The physical length, that includes the separations between segments, is 111.8 m.
[16] B.E. Carlsen and T.O. Raubenheimer, "Emittance Growth of Bunched Beams in Bends", *Phys. Rev. E 51*: 1453 (1995); Ya. S. Darbenev et al., "Microbunch Radiative Head-Tail Interaction", *DESY*, Sep. 1995.
[17] R. Assman et al., " A computer program for linear accelerator simulations", SLAC/AP-103, Oct. 1996.
[18] The simulations of longitudinal dynamics in the linac were performed with the coputer code LiTrack, written by K.L.F. Bane (SLAC).
[19] For a review of the SASE-FEL Physics, see J.B. Murphy and C. Pellegrini,"Introduction to the Physics of FELs", in *Laser Handbook*, Vol. 6, W.B. Colson, C Pellegrini and A Renieri, eds., North Holland (1990) and R. Bonifacio *et al*, *La Rivista del Nuovo Cimento*, Vol. 13, No. 9, 1990.
[20] W.M. Fawley, "An Informal Manual for GINGER and its Post-Processor SPLOTGIN", LBID-2141, Dec. 1995. CBT Tech. Note 104, UC-414.
E.T. Scharlemann, "Wiggle Plane Focusing in Linear Undulators", *J. Appl. Phys.*, **58**(6), pp.2154-2161, 1985.
T.M. Tran, J. Wurtele, "TDA3D", *Computer Phys. Commun.*, **54**, pp. 263-272, 1989.
[21] Y.H. Chin, K.-J. Kim, M. Xie, "Three-dimensional Free-Electron Laser Theory Including Betatron Oscillations", LBL-32329, May 1992, and *Phys. Rev*, A46, 6662 (1992).
[22] K.-J. Kim, "Undulator Interruption in High-Gain Free-Electron Lasers", LBNL report No. F6, August 1997.
[23] LCLS Design Study Report, SLAC Publication R-521 and UC-414, p. 8-43.
[24] K. Bane, C.-K. Ng, A. Chao, "Estimate of the Impedance due to Wall Surface Roughness", SLAC-PUB-7514 (1997)
[25] T. Orzechowski et al., *Phys. Rev. Lett.* **54**, 889 (1985); D. Kirkpatrick, *Nucl. Instr. And Meth.* **A285**, 43 (1989); J. Gardelle, J. Labrouch and J.L. Rullier, *Phys. Rev. Lett.* **76**, 4532 (1996).
[26] R. Prazieres et al., *Phys. Rev. Lett.* **54**, 889 (1985); M. Hogan et al. *Phys. Rev. Lett.* **80**, 289 (1998); M. Babzien et al.,"Observation of Self-Amplified-Spontaneous-Emission in the Near-Infrared and Visible", to be published in Phys. Rev. E; D.C. Nguyen et al., "Self-Amplified-Spontaneous-Emission Driven by a High-brightness Electron Beam", to be published in Phys. Rev. Lett.
[27] M. Hogan et al., *Phys. Rev Lett.*
[28] J. Rossbach, Private Communication.
[29] For the complete list of collaborators, see the LCLS Design Report, SLAC-R-521, p.i.